Mini-Magnetospheric Plasma Propulsion (M2P2)
NIAC Award No. 07600-010
Final Report: May 1999

R. M. Winglee
Geophysics Program
University of Washington
Seattle, WA 98195-1650
(e-mail: winglee@geophys.washington.edu)

Abstract:

Mini-Magnetospheric Plasma Propulsion (M2P2) is an advanced plasma propulsion system that will enable spacecraft to attain unprecedented speeds for minimal energy and mass requirements. The high efficiency and specific impulse attained by the system is due to its utilization of ambient energy, in this case the energy of the solar wind, to provide the enhanced thrust. Coupling to the solar wind is produced through a large-scale magnetic bubble or mini-magnetosphere generated by the injection of plasma into the magnetic field supported by solenoid coils on the spacecraft. This inflation is driven by electromagnetic processes so that the material and deployment problems associated with mechanical sails are eliminated.

Because all the enabling technology is presently available, the proposed work could have almost immediate and monumental impact on NASA's long range strategic plans for missions out of the solar system and between the planets. Specifications and proposed plans for assembling and testing of a prototype suitable for an Interstellar Precursor Mission are given. For a nominal configuration utilizing only solar electric cells for power, the M2P2 will produce a magnetic cloud approximately 15 – 20 km in radius, which would accelerate a 70 – 140 kg payload to speeds of about 50 – 80 km/s. This system would require only a few kilowatts of power to support the solenoid field coils and the plasma injection, and only a few tens of kilograms of propellant is needed. Successful testing of the system would revolutionize exploration of the solar system with its unprecedented mobility while utilizing only solar electric cells. If larger electric systems become available that could provide ten of kilowatts of power or if the power is augmented by a 100 W radioisotope system then speeds in excess of 100 km/s can be attained.

The work supported in the 6 month Phase I was focused in three areas:

(1) Specification of the overall design parameters and identify all components of the enabling technology that would be required for the M2P2,
(2) Numerical simulation of the physical processes governing the deployment of the mini-magnetosphere and the quantitative determination of the plasma and energy requirements to sustain the system and the total force that the system can achieve, and
(3) Design of a laboratory prototype that could be used in the future to validate the fundamental principles of the M2P2 system.

2. Overall Design Parameters

The basic objective of the M2P2 system is to deflect the solar wind particles by a large magnetic bubble whose field lines are attached to the spacecraft. As the charged particles of the solar wind are reflected by the magnetic field the force that they exert is transmitted along the fields lines to the spacecraft to produce its acceleration, as illustrated in Figure 1. In order to produce this coupling, the M2P2 system has basically two components: (1) a relatively strong (~ 700 G) magnetic field on the spacecraft, (2) plasma injected from the spacecraft to inflate the magnetic field and (3) a power source sufficient to generate the magnetic field and plasma. It is the combination of magnetic and plasma effects which makes the M2P2 system both unique and innovative. In particular, a current

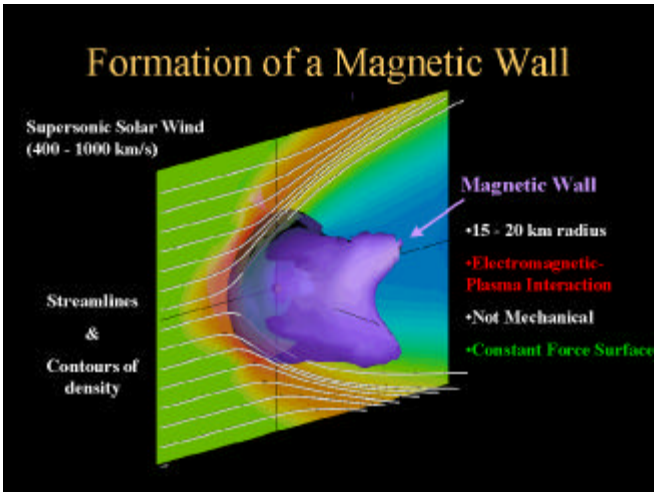

Figure 1. Schematic (based on simulations results) showing the deflection of the solar wind by a magnetic wall or mini-magnetosphere. Plasma is injected into a moderately strong magnetic field supported by field coils on the spacecraft. The injection produces the inflation of the magnetic field to form the mini-magnetosphere. This magnetic field is able to deflect the solar wind particles with speeds of 400 – 1000 km/s, as seen by the white streamlines. The color contours display plasma density with red indicating the pileup of solar wind plasma. The size of the system is determined by pressure balance between of the M2P2 system and the solar wind dynamic pressure – it is not limited by mechanical structures.

loop by itself can only produce a magnetic field that decreases as R^{-3}. Within about 10 loop radii, the magnetic field is essentially zero and the interaction region with the solar wind is very restricted, and hence inefficient. However, with the injection of plasma, the plasma can drag the magnetic field outwards once it moves into a region where the thermal and/or dynamic plasma pressure exceeds the magnetic pressure. As a result the magnetic field can fall off very much more slowly than for a simple dipole, thereby facilitating much more efficient coupling to the solar wind. The exact same processes are responsible for the formation of the heliopause where solar wind drags or convects magnetic fields from the Sun that causes the deflection of both the interstellar medium and cosmic rays. Another example is the formation of the Earth's magnetotail where R^{-1} falloffs in the magnetic field are observed.

1.1 Magnetic Field Specification

The magnetic field strength (B_{coil}) must satisfy two conditions. First, it must be sufficiently strong to ensure that the plasma ions are magnetized, i.e. the width of the plasma source (R_{plas}) must be at least a few ion gyroradii. Second, the radius of the solenoid (R_{coil}) must be several times the width of the plasma source to ensure that the ions remain magnetized as they leave the plasma source. Under these conditions, the injected plasma will flow along the field lines until the point is reached where the speed of the plasma V_{plas} matches the local Alfven speed $V_A(\mathbf{x})$. This condition equivalent to having the dynamic plasma pressure equal to the magnetic pressure (i.e. $\rho V^2 = B^2/\mu_0$). At this point, hereafter referred to as the expansion point $R_{expand,}$ the plasma can drag the magnetic field. If the plasma were to expand freely at this point then the magnetic field would decrease as R^{-2}, assuming that the magnetic field is frozen into the plasma. However, because it is confined by the force of the solar wind, large scale current sheets are produced so that the magnetic field falloff is closer to R^{-1}. The simulations in Section 2 quantitatively demonstrate this point.

If it is assumed that the dragging of the field lines occurs very close to the coil (i.e. $V_A(R_{coil})/ V_{plas} \sim 1$) then the relationship between the minimum field strength required to support the system and the system size is given approximately by

$$R_{MP} = (B_{min}/ B_{MP}) R_{coil} \quad (1)$$

where B_{MP}, is the magnetic field strength that is required to deflect the solar wind (i.e. the magnetopause field strength) and R_{MP} is the distance to the magnetopause along the Sun-satellite line.

For a solar wind density of 6 cm^{-3} and a speed of 450 km/s, the solar wind dynamic pressure is equivalent to 2 nPa. A magnetic field with B_{MP} = 50 nT is sufficient to produce an equivalent pressure of 2 nPa and hence be able to deflect the solar wind. In the following we will assume that R_{plas} is 2.5 cm and R_{coil} is 10 cm. For these parameters, the minimum coil field strength is about 0.015 T (150 G) in order to produce a mini-magnetosphere of about 15-20 km in size. The total force that would be exerted on such a system would be about 2.5 - 5 N. As noted above, if $V_A(R_{coil})/ V_{plas} > 1$, then the dragging of the magnetic field occurs further away from the coil where the magnetic field is weaker. In order to produce the same total expansion, the field strength at the coil has to be increased. The numerical results suggest empirically that the coil strength has to be increased by

$$B_{coil} \sim (V_A(R_{coil})/ V_{plas})B_{min} \quad (2)$$

The field strength for a long solenoid is given by

$$B_{coil} = \mu_0 N I/ L_{coil} \quad (3)$$

where N is the number of turns per unit length, I is the current and L_{coil} is the length of the coil. The required electrical power is $P_{el} = r_{res} L_{wire} I^2$ where r_{res} is the resistance per unit length of the wire and L_{wire} is the total length of the wire. Thus, the relationship between the required electrical power, the coil field strength, and the physical properties of the solenoid is given by

$$P_{el}^{1/2} = (2\pi/\mu_0) B_{coil} r_{res}^{1/2} (L_{coil} R_{coil} / L_{wire}^{1/2}) \quad (4)$$

There is some latitude in choosing the coil parameters depending on whether the main limitation is the weight of the system or the maximum electrical power available. As an illustrative example we will assume that the coil is restricted to a weight of 10 kg. For 10 gauge Al wire, r_{res} = 0.0053 Ω/m and L_{wire} would be 700 m. While the equivalent Cu wire has lower resistance it has proportionally more weight so that Al would be the optimum choice. In this case (4) reduces to

$$P_{el}^{1/2} = 1.4 \times 10^4 B_{coil} L_{coil} R_{coil} \quad (5)$$

For optimum power considerations, $L_{coil} \sim 2 R_{coil}$ so that for the above parameters only about 16 W would be required to produce B_{min} = 150 G. In reality, $V_A(R_{coil})/ V_{plas}$ is of the order of 5 so that B_{coil} will be about 600 G and the required power would be about 300 W. Less power would be required if more weight or equivalently L_{wire} were increased. Thus, the required magnetic field can be attained with existing technology. Use of superconducting wire can reduce the power requirements albeit at the expense of additional weight.

1.2 Plasma Specification

The inflation of the magnetic field is simplified considerably if the plasma can be produced in the high field solenoidal region of dipole field coils. The plasma will then be magnetized in the field that is to be expanded. For the plasma to stretch the magnetic field, the plasma pressure (or equivalently energy density) generated by the source must be a non-negligible fraction of the magnetic field energy. The ratio of these energies is referred to as

the plasma β and, as will be shown later, an initial β ~ 1- 4 % (or equivalently $V_A(R_{coil})/ V_{plas}$ ~ 5 - 10) in the high field solenoidal region of the dipole field is desired to expand as large a field as possible. For field strengths of the order of a 1 kG, a 1% β implies a 5 eV plasma (typical of discharges), and a density of $5x10^{13}$ cm^{-3}. There are few plasma sources that work in the presence of a strong magnetic field, and even fewer capable of producing the high density required. Plasmas generated using electrodes cannot tolerate the high heat load at the high energy densities. There are however inductively produced plasma sources (e.g. helicons) that not only produce high density discharges but do it in the presence of kilogauss magnetic fields.

With the generation of the magnetic field, plasma will be injected onto the field lines to produce its inflation. The system for generating the plasma developed from support of the Phase I grant is shown in Figure 2 [see also Section 3]. Propellant (e.g. either helium or argon) is fed through the copper pipe (seen in the lower middle) into a quartz tube. A helicon (or helix) antenna is embedded between the walls of the quartz tube so that it is physically isolated from the plasma to avoid shorting of the antenna. RF power is driven through the antenna to produce an RF breakdown of the propellant, producing plasma which flows out either end. This configuration has been chosen because it allows loading of both ends of the field lines simultaneously with the one device and thereby provides optimum efficiency, particularly with the energy densities attainable in a helicon. In addition, injected plasma returning to the spacecraft is not lost but can flow through the system or be reflected back out by the strong magnetic field within the solenoid itself. Essentially the helicon removes complexities arising from plasma/spacecraft interactions. The length of the helicon will be set by the requirement that both ends are exposed to space. Magnetic field coils that encompass the quartz tube produce the necessary magnetic field that will be inflated to produce the mini-magnetosphere.

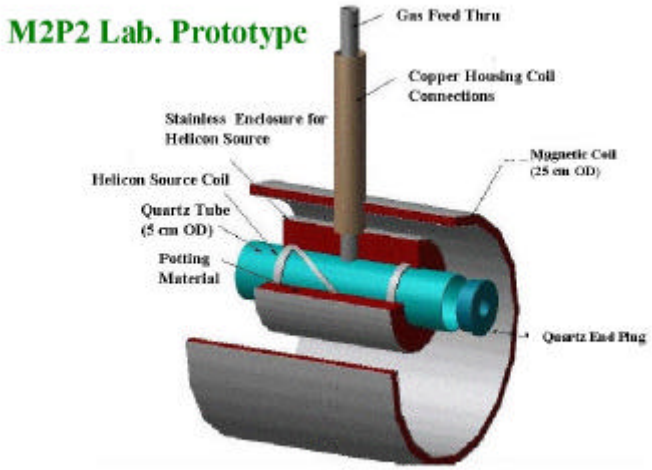

Figure 2. An early schematic of the helicon being developed at the University of Washington under Phase I support. Pictures of the actual device in operation are shown in Section 3. The helicon consists of an open-ended quartz tube into which gas, He, Ar or Xe, is injected down the center for optimum plasma production. A helix-shaped antenna is wrapped around the quartz tube to the produce radio frequency RF heating of the gas to create the plasma.

In existing experiments with laboratory helicons, the discharges are produced in solenoidal coils with axial fields from a few hundred to 1200 G. The working gas is typically argon and steady-state peak plasma electron densities up to 10^{14} cm^{-3} have been obtained in devices with diameters up to 5 cm [*Miljak and Chen,* 1998; *Gilland et al*., 1998]. These devices typically use 600 W to 1 kW RF power to produce argon ions and electrons with temperatures of about 4 eV [*Conway et al.,* 1998]. These plasma conditions are equivalent to about 40 mN of force utilizing about 7.5 $x10^{-6}$ kg/s or about 0.6 kg/day. With the bulk speed of the argon being about 3 km/s these devices produce about 120 W of plasma power.

These results can be scaled to that being proposed for the M2P2 by noting that the plasma is generated by the RF heating of ambient electrons through whistler wave-particle interactions and the subsequent ionization of the

neutral gas by the heated electrons. The ions, once formed, are accelerated along the field lines through ambipolar electric fields created by the expansion of the heated electrons. Since the plasma is produced by whistler wave interactions, the relationship between the plasma density and magnetic field strength in a helicon is given by the whistler dispersion equation

$$\frac{k^2 c^2}{\omega^2} \cong \frac{\omega_{pe}^2}{\omega(\Omega_e \cos\theta - \omega)} \qquad (6)$$

where θ is the angle between the wave vector and the magnetic field, and Ω_e and ω_{pe} are the electron cyclotron and plasma frequencies, respectively [*Shamrai and Taranov*, 1996]. For frequencies much less than the cyclotron frequency, (6) reduces to

$$\omega = \frac{k \cdot k_{||} B}{\mu_0 e n} \qquad (7)$$

For the laboratory helicons, the parallel wavelength was observed to be about 30 cm or about twice the length of the antenna [*Gilland et al.*, 1998] so that $k_{||} \sim 21\ m^{-1}$. The perpendicular wavelength is approximately equal to the 5 cm radius of the helicon, i.e. $k \sim 126\ m^{-1}$. For a 1000 G magnetic field and a wave frequency of 13.6 MHz, a corresponding density of about $1.5 \times 10^{13}\ cm^{-3}$ is predicted by (7), consistent with the observed densities. The corresponding Alfven speed is about 90 km/s and consequently $V_A / V_{plas} \sim 15$.

The most efficient operation for the M2P2 occurs when V_A / V_{plas} is fractionally above unity. To achieve this reduce ratio the proposed M2P2 system will be made more compact with the helicon antenna being about 10 cm in length and 5 cm in diameter. For a magnetic field strength of 600 G, a density of about $3.5 \times 10^{13}\ cm^{-3}$ can be attained with the same wave frequency. With the decrease in magnetic field strength and increase in density $V_A \sim 35$ km/s and $V_A / V_{plas} \sim 6$. About 350 W of electrical power and 0.75 kg/day of argon would produce this plasma.

Argon is not necessarily the best propellant for our application. While the fuel consumption is certainly better than a xenon source, it is still fairly high. A 30 kg source at the above rate would last only 40 days of continuous operation. A second concern with the use of heavy propellants is that their large mass gives them a larger gyro-orbit for a fixed energy and hence will allow them to become more easily demagnetized and lost from the system.

Light propellants such as helium can produce the same size magnetosphere for less mass and possibly with reduced mass loss from the system, albeit at higher electric power requirements. The latter is more than compensated by the fact that the reduced fuel consumption allows the M2P2 to be operated over substantially longer times and higher speeds can be attained. In particular, if helium were utilized with the same wave frequency, and the ions attain the same energy, then $V_A \sim 111$ km/s, and $V_{plas} \sim 10$ km/s. Even if all the energy of the ions is converted to thermal energy, their gyroradius at the weakest part of the magnetic field (50 nT) would be equal to about 7 km. Since this is smaller than the size of the magnetosphere, the ions are expected to remain magnetized. With a helium propellant the mass flux is reduced to 0.25 kg/day with the energy requirement increased to about 1 kW.

1.3 Acceleration Period and Spacecraft Speed

The above results show that the enabling technology required to meet the mass and energy budget for the M2P2 system is available now. The acceleration produced by this system can produce unprecedented speeds for a spacecraft. We are able to do so because, in effect, the M2P2 facilitates the exchange of low energy propellant with the high-speed solar wind. As such the few tens of milli-newtons of force required to inflate the mini-magnetosphere is able to intercept nearly a few newtons of force from the solar wind.

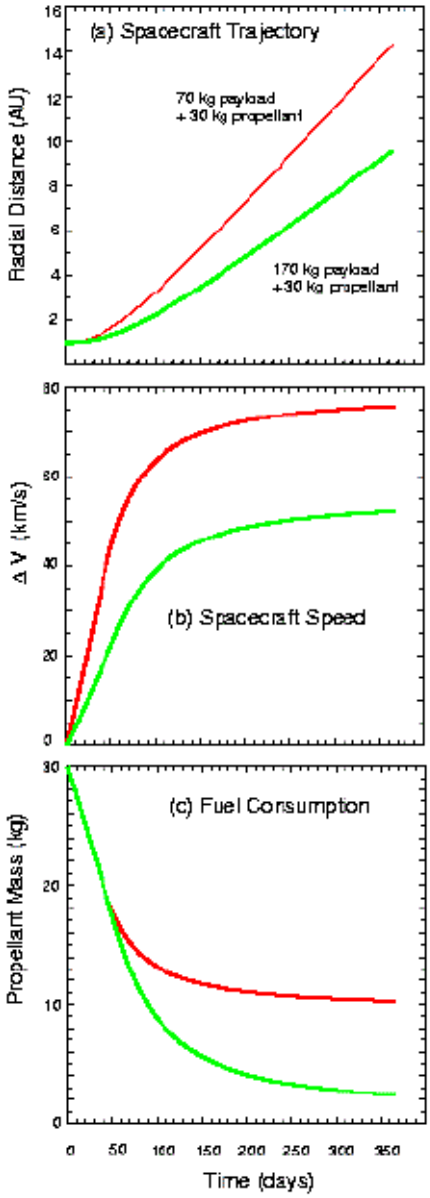

Figure 3. The trajectory, speed and fuel consumption for the M2P2 system assuming 1 N, a fuel consumption of 0.25 kg/s when the device is on and a R^{-2} decrease in power with R_{cutoff} = 1.4 AU.

The exact final velocity attained by the spacecraft is dependent on the power configuration and the chosen propellant and its mass. For the purpose of the prototype we will assume that the same electrical power is available as for Deep Space 1, i.e. 2.5 kW at 1 AU. If helium is used as the propellant then the spacecraft can move out to R_{cutoff} = 1.4 AU before the electrical power falls below that required by the M2P2 system to operate. Beyond R_{cutoff}, the M2P2 system has to be run in pulsed mode with a duty cycle of $(R_{cutoff}/R)^2$. This restriction to available power is the main limitation to the spacecraft speed.

The acceleration curves are shown in Figure 3 for the M2P2 system assuming that R_{cutoff} = 1.4 AU and that 1 N of force from the solar wind is intercepted. Two cases are shown: Case A in which the spacecraft has 100 kg mass (70 kg payload and 30 kg propellant) and Case B the spacecraft mass is 200 kg (170 kg payload and 30 kg propellant). In the two cases speeds of 50 to 75 km/s are attained. These speeds are well above anything that has previously been flown.

Moreover they are in the exact range which is required for an interstellar precursor mission. For even a fairly heavy payload of 170 kg, the M2P2 system will still be able to move the spacecraft at nearly 10 AU per year.

Furthermore these speeds are attained with nothing but solar electric propulsion. This means that a flight of the prototype could be readily done without further technical developments. With increases in available power and/or the use of superconducting magnets speeds in excess of 100 km/s can be attained.

In both the above cases the falloff in speed is due to the decline in the power available from the solar cells. With a successful flight of the prototype there would be enough motivation for the use of alternate power supplies such as a radioisotope system. Such systems are required to power any kind of scientific instruments at 100 AU, and are being used for the Cassini mission to Saturn, albeit at lower power output. For the M2P2 an alternate power source of about 100 W of power operating in pulsed mode with a 10% duty cycle would enable a 150 kg payload with 50 kg of propellant to attain a speed or nearly 100 km/s.

2. Multi-Fluid Simulations

The previous sections show that the inflation of the M2P2 system is technically feasible with all of the enabling technology readily available at this time. In this section we use multi-fluid simulations to show that the M2P2 system can be inflated with the injection of low energy plasma and produce the required deflection of the more energetic solar wind plasma at distances very much larger than would be expected from a simple dipole magnetic field. The 3-D simulations are also important because in the calculations in Section 2 essentially all the plasma is assumed to be lost. Thus, the fuel consumption rates in section 2 represent a maximum estimate. The 3-D simulations incorporate losses from the mini-magnetosphere due to (1) leakage of plasma across the magnetopause and/or (2) convection of plasma downstream into the tail of the mini-magnetosphere.

These simulations show that the estimates in Section 2 for the force needed to sustained the mini-magnetosphere are actually overly pessimistic and that as little as a few mN of force is required to sustain the system and intercept a force of about 1 N from the solar wind. This leverage of force is the innovative feature of the M2P2 system and and it is key to producing high-speed acceleration of the spacecraft with very modest power and mass requirements.

The numerical model is the same as used by *Winglee* [1998a,b] for modeling the terrestrial magnetosphere (earlier versions as applied to the magnetosphere and to the formation of stellar jets are given in *Winglee et al.* [1996], and *Goodson et al.* [1997], respectively. A multi-fluid treatment is used so that the dynamics of the solar wind plasma can be separated from the dynamics of the injected plasma inflating the magnetosphere. While the overall configuration is very similar to that derived from single-fluid MHD, the multi-fluid treatment enables the change in momentum due to the deflection of the solar wind by the magnetic barrier to be explicitly calculated. Thus, the net force on the spacecraft can be determined from the simulations by conservation of momentum.

.

3. 1. Numerical Algorthim

MHD is based on the fluid equations for plasmas but the equations for conservation of mass and energy are combined to give a single-fluid treatment. Our multi-fluid treatment is based on the same equations, but the dynamics of the electrons in the different ions species are kept separate. Specifically for electrons, it is issued and that they have sufficiently high mobility along with the lines that they are approximately in steady-state (i.e. d/dt ≅ 0) or drift motion so that the momentum equation for the electrons reduces to

$$\boldsymbol{E} + \frac{\boldsymbol{V}_e \times \boldsymbol{B}}{c} + \frac{\nabla P_e}{e n_e} = 0 \qquad (8)$$

Equation (8) is equivalent to the modified Ohm's law with Hall and grad P corrections included. The rest of the electron dynamics is given by assuming quasi-neutrality, and applying the definitions for current, and electron pressure, i.e.,

$$n_e = \sum_i n_i, \quad \boldsymbol{V}_e = \sum_i \frac{n_i}{n_e}\boldsymbol{V}_i - \frac{\boldsymbol{J}}{e n_e}, \quad \boldsymbol{J} = \frac{c}{4\pi}\nabla \times \boldsymbol{B} \qquad (9)$$

$$\frac{\partial P_e}{\partial t} = -\gamma \nabla \cdot (P_e \boldsymbol{V}_e) + (\gamma - 1)\boldsymbol{V}_e \cdot \nabla P_e \qquad (10)$$

Substituting the modified Ohm’s law (8) for the electric field into the ion momentum equation yields

$$\rho_\alpha \frac{dV_{\|\alpha}}{dt} = -(\nabla P_\alpha)_\| - \frac{n_\alpha}{n_e}(\nabla P_e)_\| \tag{11}$$

$$\rho_\alpha \frac{dV_{\perp\alpha}}{dt} = en_\alpha\left(\frac{V_\alpha \times B}{c} - \sum_i \frac{n_i}{n_e}\frac{V_i \times B}{c}\right) + \frac{n_\alpha}{n_e}\left(\frac{J \times B}{c} - (\nabla P_e)_\perp\right) - (\nabla P_\alpha)_\perp \tag{12}$$

where the || and ⊥ subscripts indicate components parallel and perpendicular to the magnetic field, respectively. For plasmas with a single ion component, (12) reduces to the MHD momentum equation.

To remove high-frequency cyclotron oscillations, the different ion species are assumed to have the same drifts across the field line, i.e.,

$$\boldsymbol{V}_\perp = \sum_i \rho_i \boldsymbol{V}_{i,\perp} / \sum_i \rho_i \ . \tag{13}$$

This approximation is the same as assumed in MHD and allows the perpendicular ion momentum to be simplified to

$$\sum_\alpha \rho_\alpha \frac{dV_{\perp\alpha}}{dt} = \left(\frac{J \times B}{c} - (\nabla P_e)_\perp\right) - \sum_\alpha (\nabla P_\alpha)_\perp \tag{14}$$

where

$$\frac{\partial P_\alpha}{\partial t} = -\gamma \nabla \cdot (P_\alpha \boldsymbol{V}_\alpha) + (\gamma - 1)\boldsymbol{V}_\alpha \cdot \nabla P_\alpha \tag{15}$$

The above equations are solved using a two-step Lax-Wendroff differencing scheme [*Richtmyer and Morton,* 1967] with Lapidus smoothing on plasma properties only. The latter is required to remove unphysical grid point oscillations across sharp discontinuities such as the bow shock.

The most difficult part of simulations is in trying to get realistic scaling since the expansion produces interactions over much scale sizes 10^5 larger than the spacecraft itself. In terrestrial magnetospheric models, the bow shock is within about 13-15 R_e (where 1 R_e is the Earth radius) and the inner radius of the simulations is typically 3 R_e so that the change in scale is very much smaller. While the simulations cannot handle a 10^5 change in scale lengths they can treat a factor of 10^3 (this dynamic range is orders of magnitude larger than existing global simulation models of the terrestrial magnetosphere). This large range of scales is treated in the simulations by breaking the grid system up into a serious (9 in all) of subsystems where the grid spacing increases by a factor of two between consecutive subsystems. The smaller subsystem provides the boundary conditions in the inner regions a larger subsystem and, conversely with the larger subsystem, provides the out of boundary conditions the smaller subsystem. This nesting of subsystems allows us to have high spatial resolution around the spacecraft while still allowing resolution of the reflection of the solar wind particles at the bow shock of magnetosphere to be fully resolved.

In the simulation results presented the subsystems consist 50x40x40 grid points with the spacecraft being represented by a sphere with a radius a 5 grid points. If it is assume that the largest subsystem represents 10 km then the inner radius represents a 10 m region around the spacecraft with a grid resolution of 2 m around it. The solar wind is assumed to have nominal values of 500 km/s and density of 6 cm^{-3} while the spacecraft is assumed to have initially only a weak (1000 nT) magnetic field. The simulations are then run for about four-transit times (0.4s)

thereby enabling solar wind to come into an approximate equilibrium with the formation of the spacecraft shock wave and wake.

Once this equilibrium has been established, the magnetic field strength is doubled and the plasma injection begins with a speed of 20 km/s such that V_A / V_{plas} = 5. The solar wind is then allowed to come into a new equilibrium. The size of the mini-magnetosphere and the change it produces in the solar wind momentum is then derived from the simulations. The process is repeated by increasing the magnetic field and the plasma density by a factor of 2 and 4 respectively, so that V_A / V_{plas} remains constant. In this manner we can thereby determine the scaling of the size of the mini-magnetosphere as a function of the solenoid field strength.

Figure 4 shows the change in size of the mini-magnetosphere for B_{coil} equal to (a) 1000, (b) 2000 and (c) 4000 nT. The contours in each panel indicate the solar wind density. For the weak magnetic field in Figure 4a, the bow shock and magnetopause are relatively close to the spacecraft. With a doubling of the magnetic field strength and associated plasma injection on the spacecraft, both the bow shock and magnetopause are seen in Figure 4b to be pushed outward almost doubling the distance. Increasing the magnetic field strength by a further factor of 2 creates another approximate doubling of the system (Figure 4c).

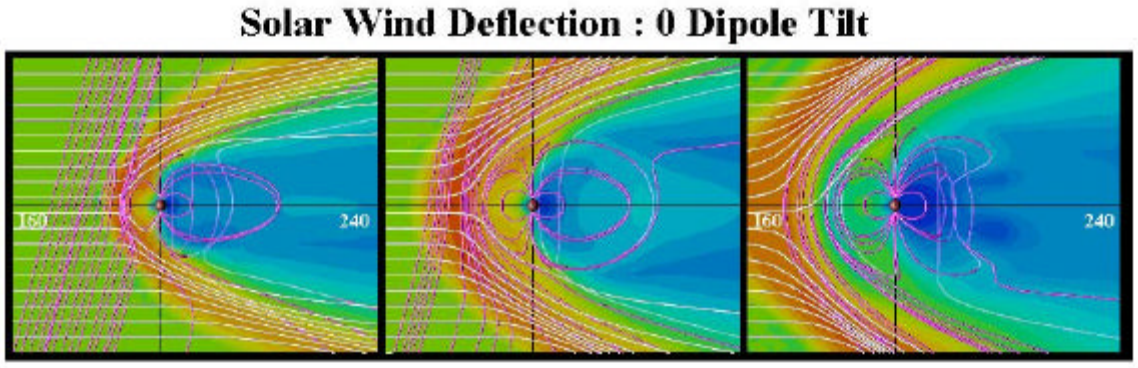

Figure 4. Inflation on the mini-magnetosphere when the magnetic axis is orthogonal to the solar wind flow. Color contours indicate the density of the solar wind with the green regions representing the undisturbed solar wind density of 6 cm^{-3}, red indicating enhancements of a factor of four as solar wind piles up around the magnetopause, and blue regions indicate depleted density in the wake with densities as small as 0.1 cm^{-3}. White lines show the flow of the solar wind around the mini-magnetosphere while magenta lines indicate the magnetic field lines. Only a subset of the simulation system is shown for clarity, extending 160 times the inner radius on upstream side and 240 times the inner radius on the downstream side (where the spacecraft is represented by it in radius of 5 grid units). The brown sphere (not to scale) indicates the position of the spacecraft

These results are suggestive that the scale size of the M2P2 is directly proportional to the strength of the magnetic field as suggested in Section 2. A test of this hypothesis is shown in Figure 5 where the solar wind profile is plotted on a scale size four times larger and where the magnetic field strength is increased by a factor of 4 from Figure 5a to Figure 5c. For greater clarity the field lines have been removed. The position of the magnetopause and bow shock pushed out approximately by the expected factor of 4.

One difference between Figure 5 and Figure 4 is that the magnetic dipole is tilted by 45^o into the solar wind. One of the main effects of this tilting is that the streamlines initially below the equator are deflected so that they pass over the spacecraft. As a result there is a net azimuthal acceleration on the M2P2. In other words, the M2P2 system is not just a drag device but lift or azimuthal acceleration can be obtained as with an ordinary solar sail by tilting the dipole.

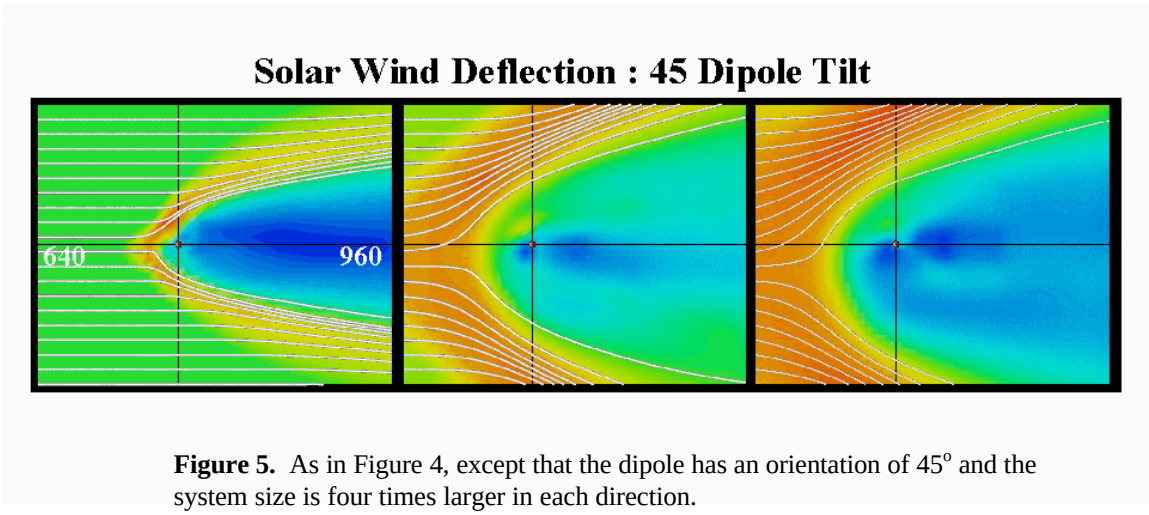

Figure 5. As in Figure 4, except that the dipole has an orientation of 45^{o} and the system size is four times larger in each direction.

The results of Figures 4 and 5 are summarized in Figure 6. The standoff distance, or equivalently the distance to magnetopause along the Sun-spacecraft line, shows more than an order of magnitude increase as the magnetic field is increased by a factor of about 20. The distance is also nearly an order of a magnitude greater than could be expected for the solar wind interaction with a simple dipole with no plasma injection. Note also that the standoff distance is used here since it is the simpler measurement, irrespective of the orientation of the dipole. However, the standoff distance is about 30% smaller than the radial cross-sectional distance. Extrapolating along the curve, the magnetic field strength that is required to produce a 15 km standoff distance (or 20 km cross-sectional distance) is about 6-7 G for our 10 m inner radius. Scaling this to a 0.1 m radius would imply that we need a magnetic field of 600-700 G on the spacecraft coils.

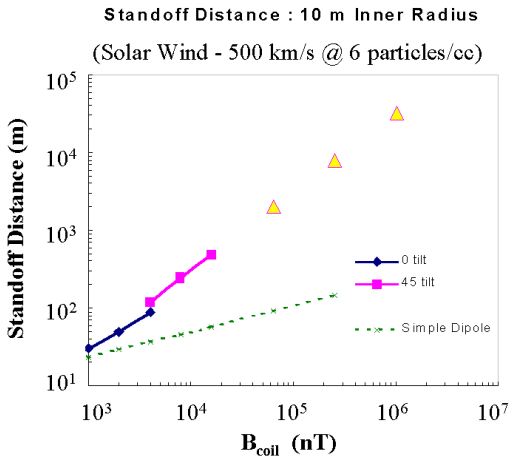

Figure 6. Size of the mini-magnetosphere as a function of coil field strength (and density of the injected plasma) for $V_A / V_{plas} = 5$ as given by the distance between the spacecraft and the magnetopause along the Sun-Earth line. The size of the inflated magnetopause is very much larger than a simple dipole, increasing almost linearly with field strength. The triangles represent extrapolation of the simulation results.

A second effect of tilting the magnetic axis into the solar wind is that the magnetosphere that is produced is actually larger. This increase in size is due to the stronger magnetic fields at the poles. The implication is that the configuration in which the magnetic axis is orthogonal to the solar wind direction is the lowest energy state and there is no danger of the solar wind blowing the M2P2 over and causing it to lose its effectiveness. Thus, higher thrust would be attainable if the dipole axis is tilted towards the solar wind, but some additional propellant would have to be expended in order to maintain its orientation.

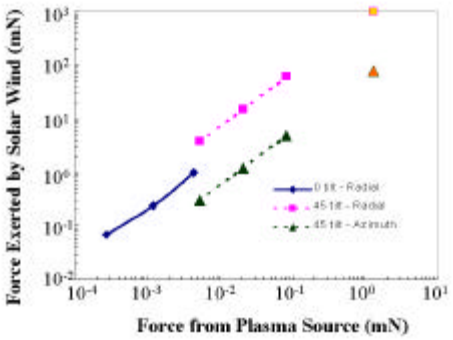

Figure 7. Force developed on the M2P2 system derived from the simulations. Because the inflation is produced by injection of low energy plasma, there is a substantial leverage of force between that required to inflate the M2P2 system and that exerted on it by the solar wind. The simulations indicate only a few mN of injected plasma is required intercept 1 N of force from the solar wind. The force is more than enough to overcome the solar gravitational force which at 1 AU is 0.6 N on 100 kg. Thus, the M2P2 system would allow the rapid escape of a spacecraft from the solar system, as indicated by the acceleration curves in Figure 3.

The total force that is imparted onto the M2P2 is shown in Figure 7. This force is calculated from the net change in the momentum flux in the solar wind plasma upstream of the M2P2 integrated through the y-z plane containing the spacecraft. There is additional force exerted on the spacecraft from the tail so the estimates described here represent a lower limit. Conservation of momentum requires that this momentum flux must be picked up by the spacecraft. It is seen that the M2P2 gives substantial leverage or multiplication factor between the force required to sustain the M2P2 and the force exerted on the spacecraft by the solar wind. Extrapolation of the simulation results indicates that in order to gain the 1 N of force on the spacecraft only about 3 mN have to be expended for a leverage of between 300 and 400.

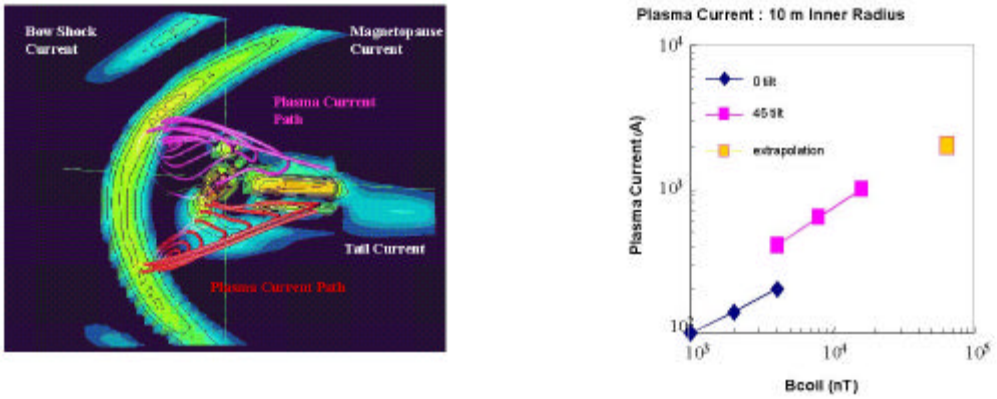

Figure 8. (a) 3-D rendering of the induced plasma current system. Contours indicate intensities in the x-z plane while the lines show the current path in 3-D for two sample regions. (b) The total induced current as a function of the coil field strength. For the M2P2 system, several to a few tens of kiloamps will be generated.

An alternative way to look at the force on the M2P2 system is through the equivalent current system produced by the solar wind interaction with the mini-magnetosphere, as illustrated in Figure 8. There are two current systems

involved. The first consists of the current loops on the spacecraft that support the dipole-like magnetic field. The injection of plasma produces the second current system in space, similar to the terrestrial current system. These plasma currents are strongest around the magnetopause and are closed by currents near the spacecraft as indicated by the line traces along the current paths.

These current paths are "D"-shaped. In the absence of outside forces the current paths should be circular. Compression into a "D" is due to the force exerted by the solar wind which is trying to pickup the plasma current system, as it would with any plasma turbulence, and convect it downstream. As it does so, the plasma currents feel the force from the spacecraft magnetic coils, and vice-versa, producing the acceleration on the spacecraft. The simulations show that several kiloamps of current will be induced by the M2P2 system. The current on the spacecraft, while only about 10 A, is driven through about a 1000 turns and therefore represents a comparable system, so that the two systems are capable of producing a force of about a Newton on each other.

3. Laboratory Prototype

In our Phase I study we exceeded our initial expectations in the proposal in that not only did we perform key numerical simulations that demonstrated the response of the device in solar wind conditions, but we also undertook the design and construction of the laboratory prototype. This latter work required:

1) attaining a vacuum chamber and restoring it to operational condition,
2) the purchasing of new turbo vacuum and roughing pumps and their installation,
3) acquisition of the RF preamplifier and amplifier and the building of matching impedance circuit for the helicon antenna,
4) the cutting and fitting of the quartz tubing and the associated plumbing for the electrical and propellant feeds,
5) fitting of the helicon antenna and its isolation from the created plasma, and
6) the turning of the magnetic field coils for the helicon geometry.

References

Conway, G. D., A. J. Perry, and R. W. Boswell, Evolution of ion and electron energy distributions in pulsed helicon plasma discharges, *Plasma Sources, Sci. and Tech.,* **7**, 337, 1998.

Forward, R. L., Grey solar sails, *J. Astronautical Sciences,* **38**, 161, 1990.

Gilland, J., R. Breun, and N. Hershkowitz, Neutral pumping in a helicon discharge, *Plasma Sources, Sci. and Tech.,* **7**, 416, 1998.

Goodson, A. P., R. M. Winglee, K.-H. Bohm, Time dependent accretion of magnetic young stellar objects as a launching mechanism for stellar jets, *Astrophys. J.*, **489**, 199, 1997.

Miljak, D. G., and F. F. Chen, Density limit in helicon discharges, *Plasma Sources, Sci. and Tech.,* **7**, 537, 1998.

Richtmyer, R. D., and K. W. Morton, *Difference Methods for Initial Value Problems*, p. 300, Interscience, New York, 1967.

Shamrai, K. P., and V. B. Taranov, Volume and surface RF power absorption in a helicon plasma source, *Plasma Sources, Sci. Tech.*, **5**, 474, 1996.

Steinolfson, R. S., V. J. Pizzo, and T. Holzer, Gasdynamic models of the solar wind/interstellar medium interaction, *Geophys. Res. Lett.,* **71**, 245, 1994.

Suess S.T., The heliopause, *Rev. Geophys.,* **28**, 97-115, 1990.

Winglee, R. M., *et al.,* Modeling of upstream energetic particle events observed by WIND, *Geophys. Res. Lett.*, **23**, 12,276, 1996.

Winglee, R. M., Multi-fluid simulations of the magnetosphere: The identification of the geopause and its variation with IMF, *Geophys. Res. Lett.* **25**, 4441,1998a.

Winglee, R. M., Imaging the ionospheric and solar wind sources in the magnetosphere through multi-fluid global simulations, *Physics of Space Plasmas*, **15**, 345, 1998b.